BLOOD FLOW NUMERICAL SIMULATION OF AN IDEALISED STENOSED ARTERY: FINITE ELEMENT METHOD AND FINITE VOLUME METHOD COMPARISON

Jayme Pinto Ortiz
Universidade de São Paulo – Escola Politécnica – Departamento de Engenharia Mecânica
Avenida Prof. Luciano Gualberto, travessa 3 nº 380 - CEP - 05508-900 - São Paulo/SP - Brazil
jportiz@usp.br
Instituto Mauá de Tecnologia – Centro Universitário – Escola de Engenharia – São Caetano do Sul
ortiz@maua.br

Kleiber Lima de Bessa
Universidade de São Paulo – Escola Politécnica – Departamento de Engenharia Mecânica
Avenida Prof. Luciano Gualberto, travessa 3 nº 380 - CEP - 05508-900 - São Paulo/SP - Brazil
kleiber.bessa@poli.usp.br

Daniel Formariz Legendre
Universidade de São Paulo – Escola Politécnica – Departamento de Engenharia Mecânica
Avenida Prof. Luciano Gualberto, travessa 3 nº 380 - CEP - 05508-900 - São Paulo/SP - Brazil
daniel.legendre@poli.usp.br

Rudolf Hellmuth de Almeida Prado
Universidade de São Paulo – Escola Politécnica – Departamento de Engenharia Mecânica
Avenida Prof. Luciano Gualberto, travessa 3 nº 380 - CEP - 05508-900 - São Paulo/SP - Brazil
rudolf.hellmuth@poli.usp.br

Abstract. *Atherosclerosis is a disease of arteries in which localized deposits and accumulation of cholesterol and lipid substances, as well as proliferation of connective tissues, cause a partial reduction in the arterial cross-sectional area (stenosis). This paper presents a computational fluid dynamics modeling for the analysis of pulsatile blood flow in idealized normal artery (no area reduction) and in axisymmetric stenosed artery (33% of area reduction). This study assumes the vessel as a rigid wall tube and the blood flow is considered to be incompressible homogeneous Newtonian fluid and axisymmetric. For modeling Dirichlet boundary conditions were applied at the inlet. A physiological waveform of the femoral artery of a dog was considered as a pulsatile velocity input and with no slip boundary conditions applied at artery wall and pressure boundary conditions applied at the outlet. Two different CFD codes were comparatively used in this case, one based on Finite Element Method (FEM) and other based on Finite Volume Method (FVM). Ansys 8.0 was used for FEM simulation and Fluent 6.2 was used for FVM simulation. The two codes application presented similar results, although the computational time for FEM analysis is much higher when compared with the computational time for FVM analysis.*

Keywords*: Stenosed Artery, Hemodynamic, Physiological Waveform, Numerical Simulation, Wall Shear Stress.*

1. Introduction

The pulsatile flow of blood through the arterial vasculature generates various types of hemodynamic forces such as wall shear stress, hydrostatic pressures, and cyclic strains that can impact vessel wall structure. Hemodynamic regulates blood vessel structure and it also influences the development of several kinds of vascular pathologies. This factor has an important function in the pathogenesis and pathophysiology of atherosclerosis (Berger and Jou, 2000). Fry (1968) suggested that regions of high shear stress, which implicates in a direct mechanical harm of the vessel wall, were regions where occurred atherosclerosis. Conversely, Caro et al (1971) stated that atherosclerosis occurs in sites of low shear stress because of low mass diffusion of lipids. Some studies have demonstrated, according with Caro theory, that intimal plaque becomes thicker in regions of low shear stress. Atherosclerosis is a disease of arteries in which localized deposits and accumulation of cholesterol and lipid substances, as well as proliferation of connective tissues, causes a partial reduction in the arterial cross-sectional area (stenosis). This disease is geometrically focal and it tends to happen in localized sites of complex geometry, such as bifurcations, junctions and high curvature regions. This disease can severally disturb hemodynamics patterns. It is also associated to low and oscillatory wall shear stress (WSS) in sites where blood flow is slow and change direction with the cardiac cycle. In the other hand, vessel sites with steady blood flow and high shear stress are comparatively disease-free.

The numerical simulation has been used to study hemodynamic behavior inside the artery vessel. Even though a stenosed artery is difficult to represent because of its varied and complex geometry, some simplification can be applied in order to facilitate numerical simulation (Marques et al, 2003). A rigid tube has been adopted in this study, considering an axisymmetric constriction. The hypothesis of a rigid tube for the vessel is not so far from reality, once the atherosclerosis promotes some reduction in the elastic properties of the vessel wall. Several studies have been

performed, in a first approximation, in rigid stenosis and most of them have adopted steady flow (Zendehbudi, 1999). Depending on the constriction severity of the atheroma, the flow behavior in the poststenotic region could be disordered and/or in transition to turbulent, although the presence of a laminar flow condition in the prestenotic site. Studies assuming axisymmetric stenosis and steady flow showed that the flow characteristics depend on Reynolds number and stenosis geometry. Long et al (2001) obtained numerical solution assuming a physiological pulsatile flow through different models of stenosis. They also assumed in the modeling rigid tube, laminar flow and Newtonian fluid. They have found that during the systolic deceleration phase there is a formation and development of flow separation zones in the poststenotic region. In addition, they have demonstrated some factors that influence the poststenotic flows, such as the severity and geometry of the stenosis and the pulse waveform of the flow.

Wall shear stress (WSS) is another important characteristic that should be considered for this study. The WSS distribution is very valuable in order to understand the consequences of flow characteristics on endothelial cells, see Fig.1. Endothelial cells of blood vessels are permanently exposed to shear stress and the range of stress in physiological normal pattern is in between 1,0 to 7,0 Pa. When these values grown up to a range higher than 10 Pa, thrombosis can occurs. For values higher that 35 Pa, direct endothelial injury and denudation occur. On the other hand, a low shear stress with values on the order of +/- 0,4 Pa is associated with atherogenesis (Malek, 1999). Sites of complex geometry, such as bifurcations or stenosis, which is predisposed to stagnation and recirculation of blood flow, can promote the atherogenisis because of the presence of low shear stress involved in these regions. In addition, blood flow through arteriovenous fistulae has showed regions of low shear stress, which was in the range of atherosclerosis occurrence (Ortiz and Bessa, 2003).

The present study was concerned with pulsatile flow in a model of a normal artery (no area reduction) and in a model of axisymmetric stenosis (33% of area reduction). A canine femoral artery blood flow waveform was assumed as an inlet condition. In this study it is intended to improve our understanding of hemodynamic in pathological and non-pathological canine artery models. Additionally, there was the intention to identify regions of atherogenesis predisposition due to situations of low shear stress.

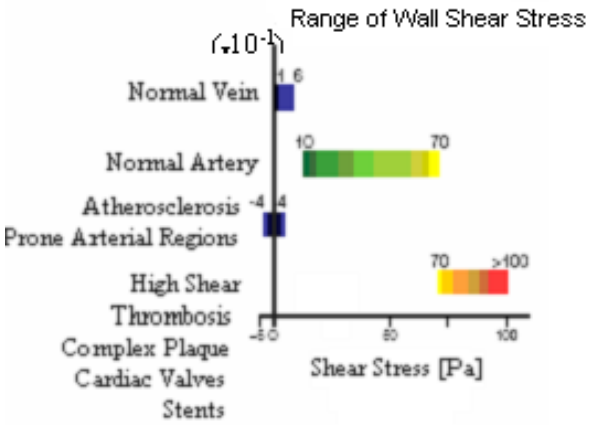

Figure 1. Range of wall shear stress in different vessels associated with different pathologies (Malek, 1999).

2. Methods

This study assumes the vessel as being a rigid wall tube and the blood flow is considered to be incompressible homogeneous Newtonian fluid and axisymmetric. Two cases have been idealized, one of a normal artery (no area reduction) and other of axisymmetric stenosis (33% of area reduction). For this model, ideal Dirichlet boundary conditions were applied at the inlet. A physiological waveform of the femoral artery of a dog was applied "Fig. 2" (McDonald, 1974). This waveform was considered as a pulsatile velocity input and with no slip boundary conditions and impermeability applied at artery wall. Constant pressure boundary condition was imposed at the outlet, which was placed far enough from entrance (normal artery) or from the constriction site (stenosed artery).

The effects of wall compliance have been neglected in this work. This hypothesis assumption is attenuated considering the arterial vessel, as a rigid tube is a simplification not so far from reality in this case, because of atherosclerosis promotes some reduction in the elastic properties of the vessel wall.

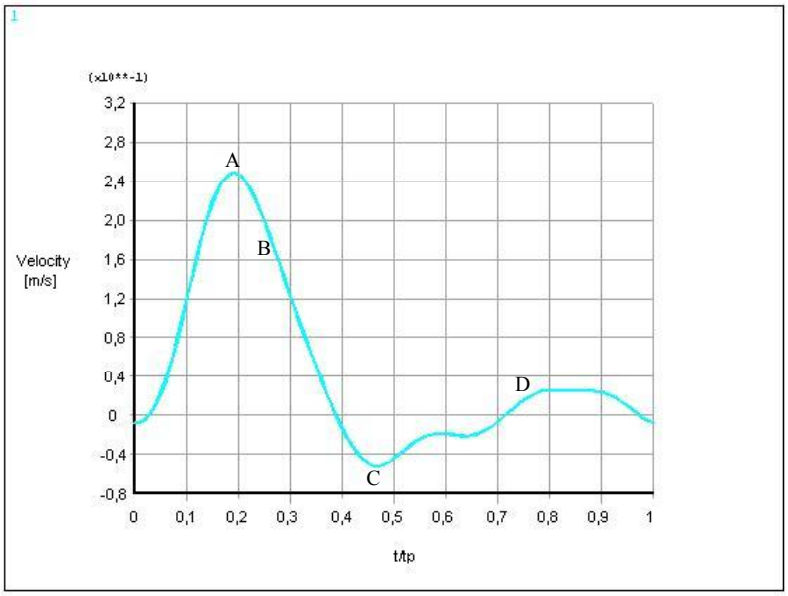

Figure 2. A typical physiological waveform of the femoral artery of a dog

A dimensionless parameter t/tp is introduced to describe a particular point in the cardiac cycle, where t is the specific instant [s] and tp is the period of the cycle [s]. The results were compared considering four different points of the inlet velocity waveform. These four elected points are showed by letters A to D in Fig. 2 and they correspond to values of the dimensionless (t/tp) of 0,19 (A), 0,25 (B), 0,47 (C) and 0,6 (D).

The governing equations are:

Mass Conservation Equation:

$$\nabla \cdot \left(\rho \vec{V}\right) + \frac{\partial \rho}{\partial t} = 0 \tag{1}$$

Momentum Conservation Equation:

$$\rho \frac{D\vec{V}}{Dt} = \rho \vec{g} - \nabla p + \mu \nabla^2 \vec{V} \tag{2}$$

where ρ is the fluid density [kg/m^3], $\vec{V}$ is the velocity vector [m/s], t is time [s], $\vec{g}$ is gravity acceleration [m/s^2], p is pressure [Pa] and μ is the dynamic fluid viscosity [Pa.s].

The flow rate and pulse were defined according to physiological parameters of Reynolds number and Womersley number. The Reynolds number is a relation between inertial and viscous forces.

$$\mathrm{Re} = \frac{VL}{\nu} = \frac{4Q}{\pi D \nu} \tag{3}$$

where V is the mean velocity [m/s], L is the characteristic length (vessel diameter), Q is the volumetric flow [m^3/s], ν is the cinematic viscosity [m^2/s] and D is the vessel diameter.

In a pulsatile flow, the pulse rate is determined by Womersley parameter (W), which relates frequency of a pulsatile wave and viscous forces.

$$W = \frac{D}{2}\sqrt{\frac{w}{\nu}} \tag{4}$$

where w is the frequency of a pulsatile wave.

According to the concept of the Stokes layer, the parameter δ_S of Stokes layer thickness or viscous wave penetration is given by:

$$\delta_S = 5\sqrt{\frac{\nu}{w}} \tag{5}$$

Fluid properties were assumed following literature (Berger, 1996). It is assumed the fluid density of 1.050 [kg/m3], the dynamic viscosity of 0,00345 [Pa.s] and the cinematic viscosity of $3{,}29 \times 10^{-6}$ [m^2/s]. The period of cardiac cycle (t_p) was taken as 0,8 seconds. The Stokes layer thickness δ_S is equal 0,0032 m, for the simulations presented.

Initial simulation were done for the two artery models under investigation, to get information in terms of grid and time step independence, which means that both were independent of the size of the element or control volume and increment in time (time step). Grid independence was achieved by using 40.000 quadrilateral elements and 77.000 control volumes and the time step independence was achieved using a time increment of 0,008 seconds.

Two different commercially available CFD codes were comparatively used in this case, one based on Finite Element Method (FEM) and other based on Finite Volume Method (FVM). For this study it were used Ansys 8.0 for FEM analysis and Fluent 6.2 for FVM analysis. The geometry of each model, stenosed and normal artery, is given in Fig. 3 II and Fig. 4 II respectively. The geometrical parameters for both models are as follows: vessel diameter and vessel length equal to 0,006 m and 0,154 m, respectively, for normal artery. Vessel diameter 0,004 m (33% of area reduction) and vessel length 0,024 m, for stenose region. The stenosis was assumed as axisymmetric. The grid was non-uniformly distributed in the axial direction with fine elements or cells in the stenosis, but uniformly distributed in axial direction in the model of normal artery. In addition, both were more refined near the vessel wall “Fig. 3 I” and “Fig. 4 I”.

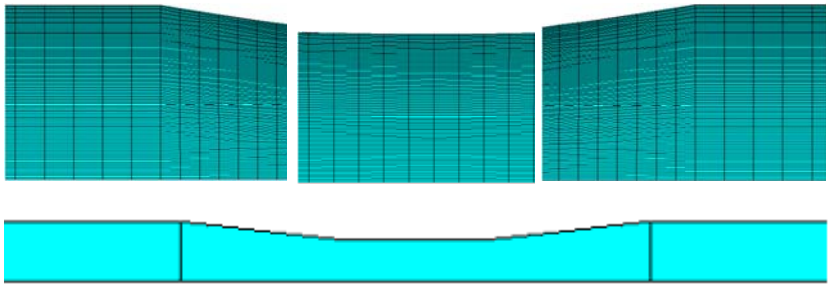

(I)

(II)

Figure 3. Discretization grid for the stenosed artery (I) and its idealized geometry (II).

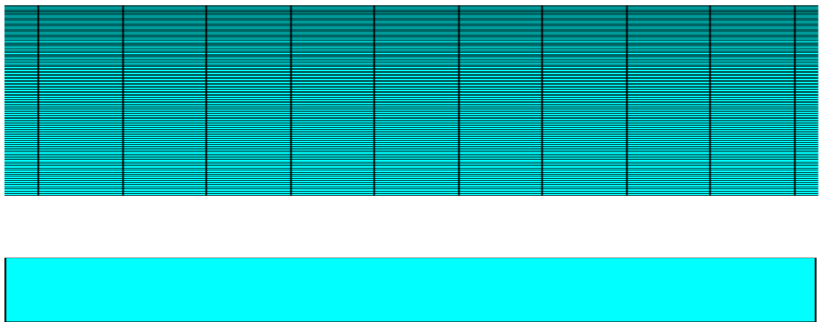

(I)

(II)

Figure 4. Discretization grid for the normal artery (I) and its idealized geometry (II).

3. Results

CFD simulations were performed for normal artery (no area reduction) and axisymmetric stenosis (33% of area reduction). Simulations results for flow including velocity field and WSS distribution obtained for the whole domain are presented at selected points (A to D) in the cardiac cycle.

Figure 5 I and II correspond to a comparison between FEM and FVM, respectively, for the normal artery model. Both have showed almost the same magnitude and feature for all points (A to D) at the cardiac cycle. It is presented a flow inversion, which occurs at the point C of the cardiac cycle (t/tp=0,47).

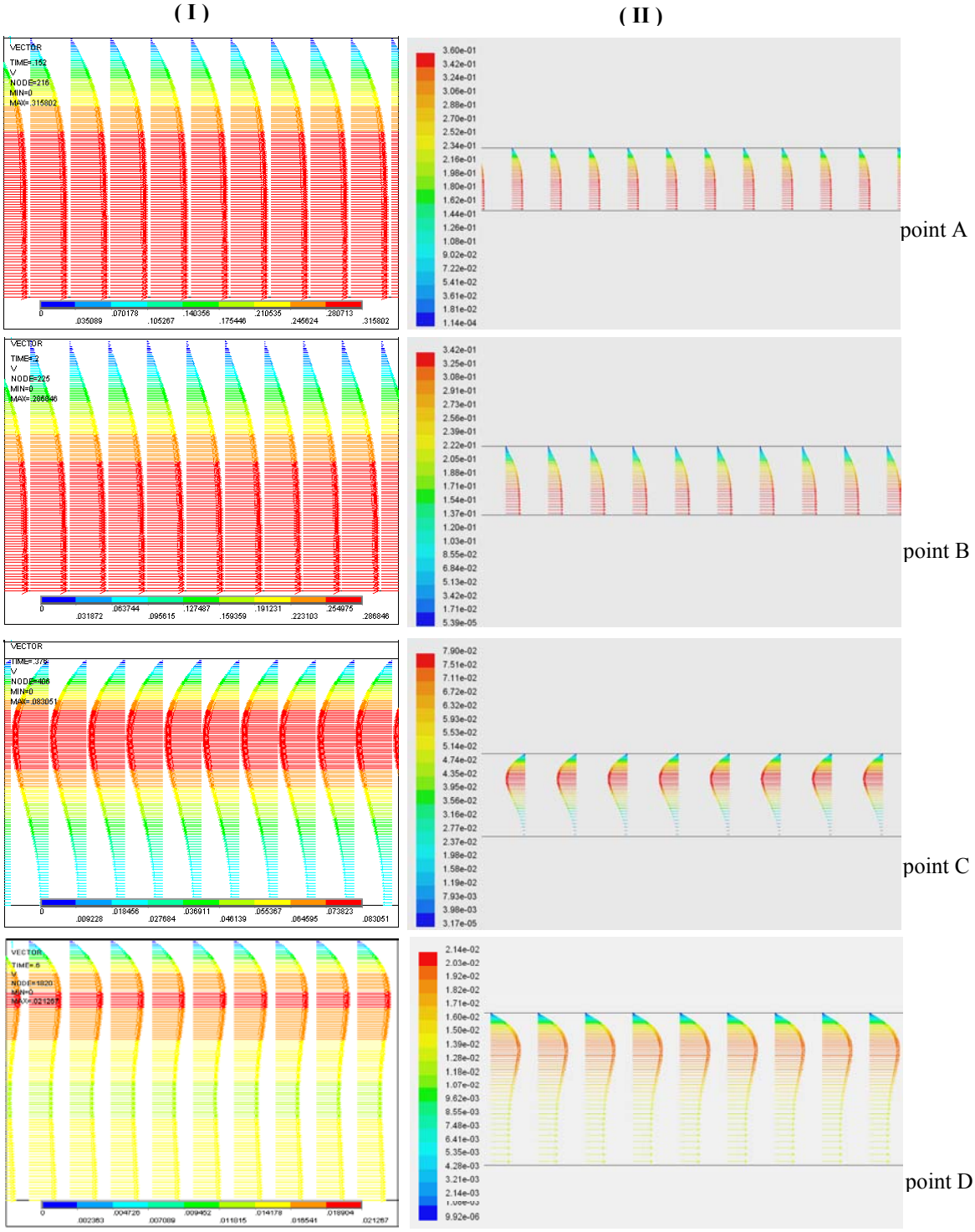

Figure 5. Comparison between FEM (I) and FVM (II) for the normal artery model at points (A to D).

The stenosed artery model have been divided in three regions in order to compare the velocity field and identify the feature flows between them, and these regions correspond to prestenotic, stenosed and poststenotic “Fig. 6 I” and “Fig. 6 II”. Figure 6 I and II correspond to a comparison between FEM and FVM, respectively, for the stenosed artery model. Both have showed almost the same magnitude and feature for the point B at the cardiac cycle. It is also presented a high velocity field at the stenosed site, but occur a reversal flow at the poststenotic region.

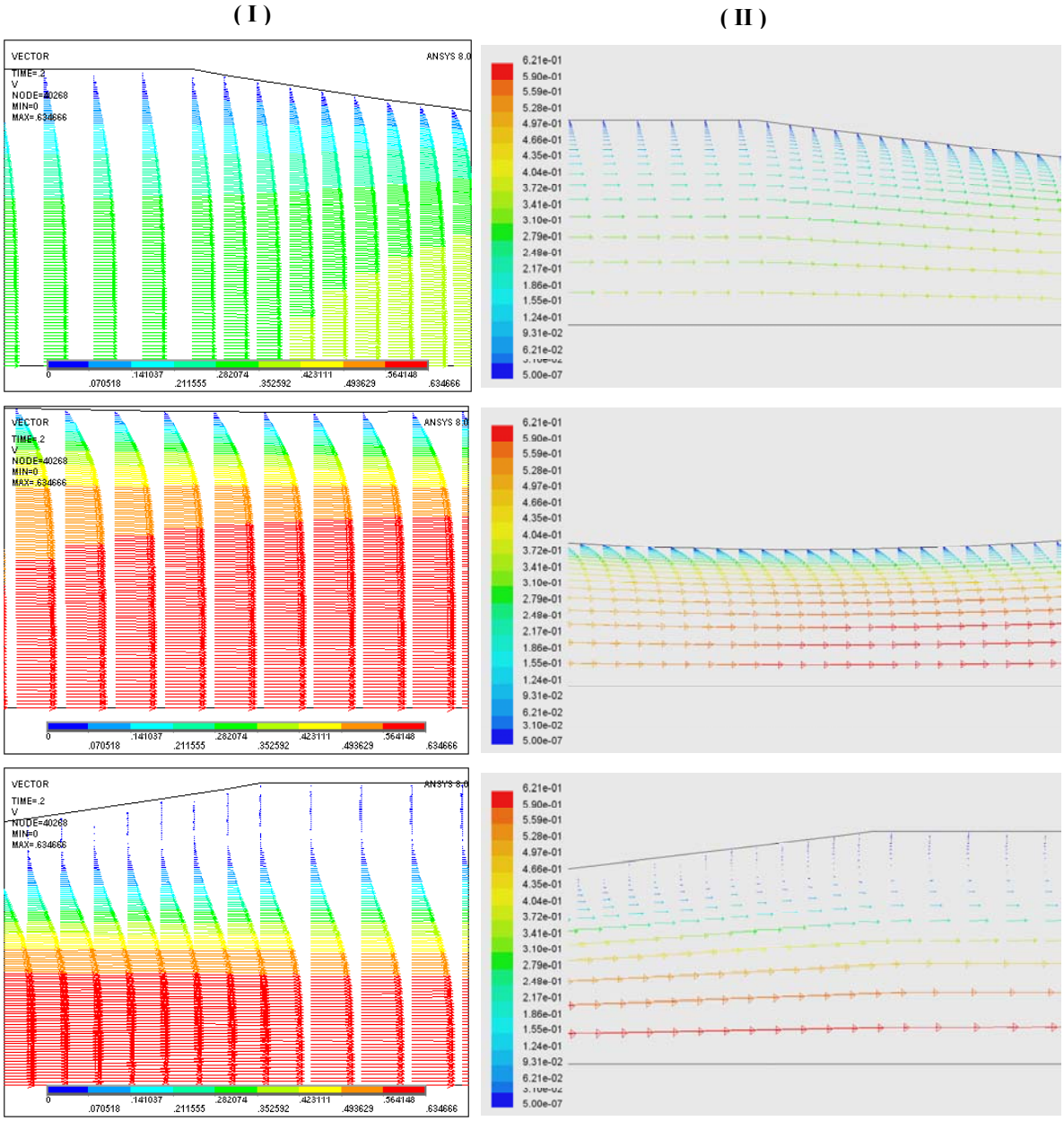

Figure 6. Comparison between FEM (I) and FVM (II) for the stenosed artery model at the point B of the cardiac cycle.

Figure 7 I and II correspond to a comparison between FEM and FVM, respectively, for the stenosed artery model. Both have showed almost the same magnitude and feature for the point D at the cardiac cycle. It is also presented a high velocity field at the stenosed site, but occur a reversal flow at the prestenotic region. It is showed the streamlines of the prestenotic region focusing the recirculation zones (III).

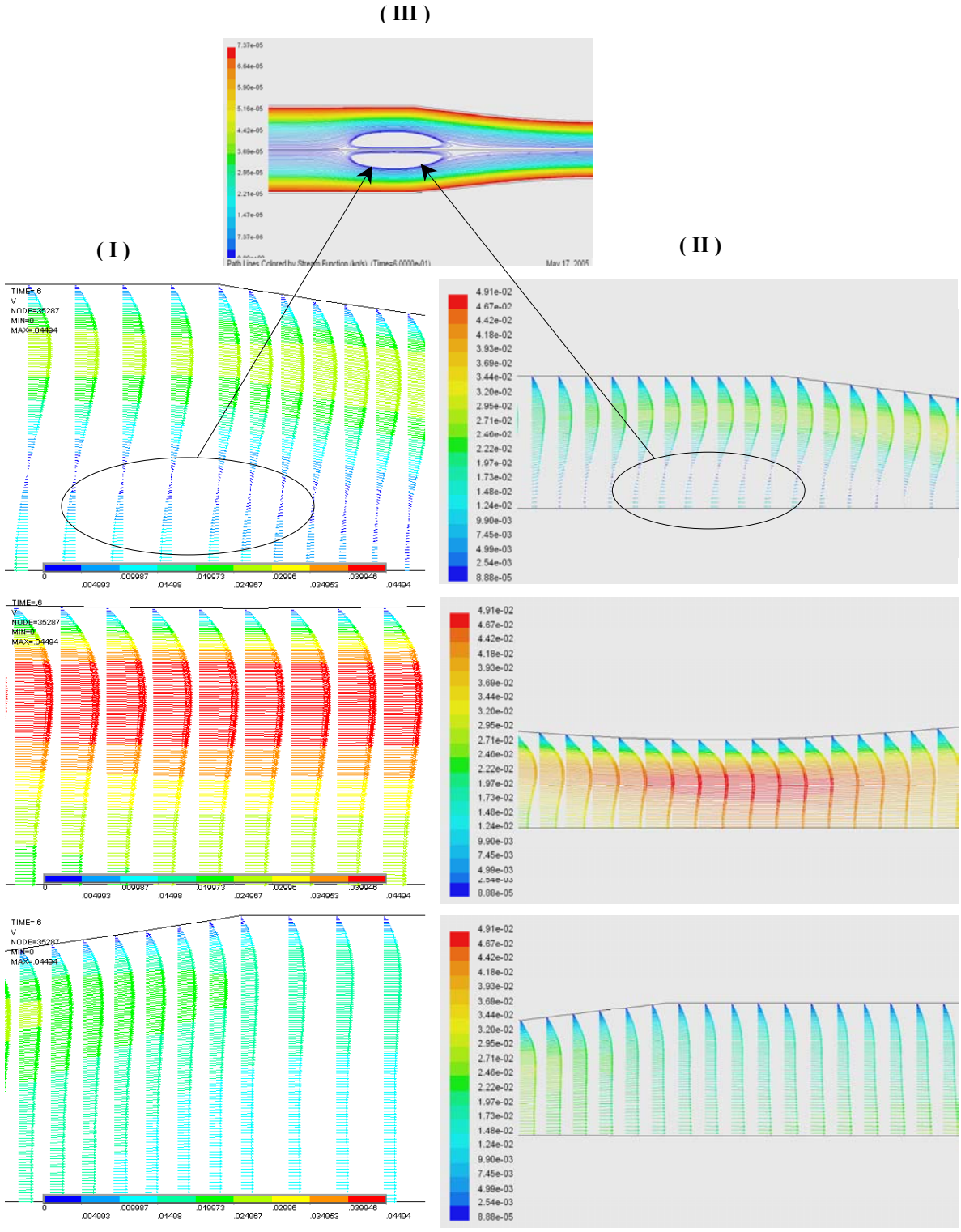

Figure 7. Comparison between FEM (I) and FVM (II) for the stenosed artery model at the point D of the cardiac cycle showing the streamlines of the prestenotic region focusing the recirculation zones (III).

Figure 8 I, II and II correspond to a comparison among a model using 40.000 quadrilateral elements for FEM analysis “Fig. 8 I”, a model using 40.000 quadrilateral volumes for FVM analysis “Fig. 8 II” and a model using 77.000 quadrilateral volumes for FVM analysis “Fig. 8 III” in all points (A to D) of the cardiac cycle for the stenosed artery model. Except for the Fig. 8 II, the others have showed almost the same magnitude for the points A, C and D. The 40.000 quadrilateral volumes model - FVM “Fig. 8 II” have presented higher values of WSS for the point B that for the

point A. However, the physiological waveform has highest velocities values at the point A, which should present higher values of WSS.

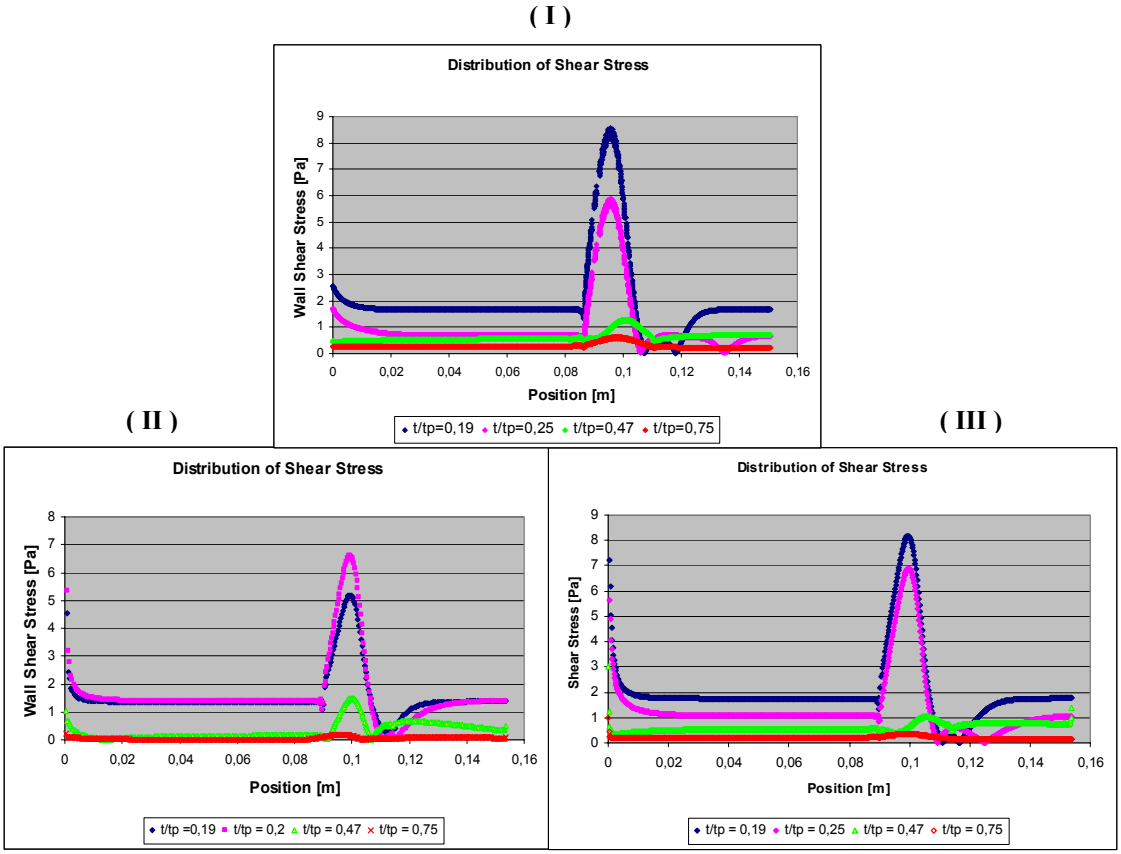

Figure 8. Comparison among distribution of wall shear stress in a model using 40.000 quadrilateral elements for FEM analysis (I), in a model using 40.000 quadrilateral volumes for FVM analysis (II) and in a model using 77.000 quadrilateral volumes for FVM analysis (III) in all points (A to D) of the cardiac cycle for the stenosed artery.

4. Conclusions

In this study, numerical results of a pulsatile blood flow through an idealized model of femoral dog artery were presented. The studied cases were performed for a normal artery and axisymmetric stenosed artery with a physiological waveform of the femoral artery of a dog. The results included time dependent velocity fields and wall shear stress distributions. In this work some hypotheses were adopted such as rigid vessel wall, incompressible homogeneous Newtonian fluid and axisymmetry.

Since the Stokes layer thickness is of the order of the radius, there is a prevalence of viscous effect in the whole domain. The results show the effect of the unsteadiness in the flow through the artery. Changes of the velocity field happen due to the development of reversal pressure gradient.

It is showed that reversal flow varies according with cardiac cycle phase. Changes the flow feature occur in magnitude and in radial position. The results are strongly time dependent, which means it is affected by the pulsatile flow. The feature of the poststenotic flow will depend on the stenosis geometry and flow characteristic.

The wall shear stress distributions have been observed for the whole domain. These values depend of axial position, cardiac cycle phase, and stenosis geometry. It is a crucial hemodynamic parameter that determines the initiation of atherogenesis. The range of shear stress in physiological normal pattern is in between 1,0 to 7,0 Pa, however, the low shear stress observed in this study is of the order of 0,4 Pa, which is associated with atherogenesis. On the other hand, the highest value of WSS found is of the order of 8,7 Pa, which is into the range of the thrombosis occurrence (higher than 7 Pa).

The 40.000 volumes model - FVM “Fig. 8 II” have presented higher values of WSS for the point B that for the point A. However, the physiological waveform has highest velocities values at the point A, which should present higher values of WSS. This was a grid dependent case that was solved by mesh refinement (77.000 volumes) of the whole model domain. However, this refined model has spent twice the time of the initial FVM model. The FEM model (40.000 elements) and the FVM model (77.000 volumes) show the same results, and although the time increasing for

FVM model refinement, the computational time is of order of three times lower when compared with FEM model computation time (40.000 elements).

5. Acknowledgements

We gratefully acknowledge the financial support of CNPq for the scholarships of graduate student Kleiber Bessa and undergraduate student Rudolf Prado.

6. References

Berger, S.A., Goldsmith, W. and Lewis, E.R., 1996, "Introduction to Bioengineering", England: Oxford University Press.

Berger, S.A. and Jou, L-D., 2000, "Flows in Stenotic Vessels", Annu. Rev. Fluid Mech., Vol. 32, pp. 347-382.

Caro, C.G., Fitz-Gerald, J.M., Schroter, R.C., 1971, "Atheroma and Arterial Wall Shear: Observation, Correlation and Proposal of a Shear Dependent Mass Transfer Mechanism for Atherogenesis", Proc. R. Soc. Lond. B. Biol. Sci, Vol. 17(7), pp. 109-159.

Fry, D.L., 1968, "Acute Vascular Endothelial Changes Associated with Increased Blood Velocity Gradients", Circ. Res., Vol. 12, pp. 165-197.

Lee, K.W. and Xu, X.Y., 2002, "Modeling of Flow and Wall Behavior in a Midly Stenosed Tube", Medical Engineering & Physics, Vol.24, pp. 575-586.

Long, Q., Xu, X.Y., Ramnarineb, K.V. and Hoskins, P., 2001, "Numerical Investigation of Physiologically Realistic Pulsatile Flow Through Arterial Stenosis", Journal of Biomechanics, Vol.34, pp. 1229-1242.

McDonald, D.A., 1974, "Blood Flow in Arteries", 2nd Ed. London: Arnold, 496 p.

Malek, A.M., Alper, S.L. and Izumo, S., 1999, "Hemodynamic Shear Stress and Its Role in Atherosclerosis", JAMA, Vol 282, No. 21, pp. 2035-2042.

Marques, P.F., Oliveira, M.E.C., Franca, A.S. and Pinotti, M., 2003, "Modeling and Simulating of Pulsatile Blood Flow with a Physiologic Wave Pattern", Artif. Organs, Vol. 27, No. 5, pp. 478-485.

Ortiz, J.P., Bessa, K.L., 2003 "Flow Simulation Through Arteriovenous Fistulae", COBEM, São Paulo-SP.

Zendehbudi, G.R. and Moayeri, M.S., 1999, "Comparison of Physiological and Simple Pulsatile Flows Through Stenosed Arteries", Journal of Biomechanics, Vol. 32, pp. 959-965.